Peer-reviewed version available at *Materials* **2018**, *11*, 2421; doi:10.3390/ma11122421

Article

Influence of gradual damage on the structural dynamic behaviour of composite rotors: Experimental investigations

Angelos Filippatos [1]* and Maik Gude [1]

[1] Institute of Lightweight Engineering and Polymer Technology (ILK), Technische Universität Dresden, Dresden, Germany; ilk@mailbox.tu-dresden.de

* Correspondence: angelos.filippatos@tu-dresden.de; Tel.: +49-351-463-39463

Abstract: Fibre-reinforced composite structures under complex loads exhibit gradual damage behaviour with a degradation of effective mechanical properties and change of their structural dynamic behaviour. Damage manifests itself as spatial increase of inter-fibre failure and delamination-growth, resulting in local changes of stiffness. These changes affect not only the residual strengths but more importantly the structural dynamic behaviour. In case of composite rotors, this can lead to catastrophic failure if an eigenfrequency coincides with the rotational speed. The description and analysis of the gradual damage behaviour of composite rotors therefore provides the fundamentals for a better understanding of unpredicted structural phenomena. The gradual damage behaviour on the example of composite rotors and the resulting damage-dependent dynamic behaviour is experimentally investigated under propagating damage for combined out-of-plane and in-plane loads. A novel observation is reported, where monotonic increase of damage results in non-monotonic frequency shift of significant amount of eigenfrequencies.

Keywords: gradual damage behaviour; damage propagation; modal properties; composite rotor; structural dynamic behaviour

1. Introduction

Composite materials provide high strength and stiffness-to-weight ratios and adjustable directional material properties. Due to such outstanding properties, an increasing interest to use composite materials in weight-relevant applications of complex-loaded structures is noticeable. Especially, constantly growing requirements for the efficiency and reliability of modern high-performance rotors for gas, steam and wind turbines as well as ventilators demand the increased application of advanced fibre-reinforced composites, as conventional materials are reaching their physical limits. Besides outstanding specific strength and stiffness properties, fibre-reinforced composites offer significant advantages regarding cost-efficient manufacturing due to the feasibility of producing very complex, near-net-shaped fibre reinforcements for rotor components. In addition, their adjustable gradual damage behaviour is advantageous – in contrast to the classical metallic materials – as it allows for the development of rotors which are characterised by a gradual damage behaviour.

Due to this gradual damage behaviour, the remaining structural strength of composite rotors is generally not reduced critically, and a structural failure will often be prevented as long as the loads do not further increase. Notably, the gradual damage strongly affects the structural vibration behaviour, which means that an altered dynamic behaviour of the composite structure can be treated as a symptom of a new damage state, which can be of major interest for advanced damage identification methods, especially for vibration-based diagnostic approaches.

1.1. Motivation

An unknown or a false understanding of the damage-dependent structural dynamic behaviour of composite rotors can lead to severe misinterpretations and false decision making. Especially in damage

Peer-reviewed version available at Materials 2018, 11, 2421; doi:10.3390/ma11122421

identification methods such as vibration-based diagnostics, a false classification of the vibration response to a damage state can result to a catastrophic failure.

The goal of the current investigations is to gain information and knowledge regarding the effect of the occurring complex damage phenomena on the structural dynamic behaviour of composite rotors. As a result, the relation between the gradual damage behaviour of composite rotors and the resulting damage-dependent structural dynamic behaviour is described and depicted as frequency shifts of selected eigenfrequencies to the increasing damage.

1.2. State-of-the-art

A thorough literature exists in the design and development of composite rotors, which partially consider the complex gradual damage behaviour of composite materials. Furthermore, fewer investigations are to be found regarding the effect of the gradual damage behaviour on the structural dynamic behaviour of composite rotors. Even fewer are the publications that investigate complex, non-monotonic changes of the structural dynamic behaviour, such as the modal properties, due to damage increase.

Gradual damage behaviour of composites

The increasing application of composite materials has led to numerous investigations on the gradual damage behaviour of composites e.g. [1–4]. These investigations reveal that the gradual damage behaviour of composites is governed by a mixture of various fracture modes, e.g. inter-fibre failure, fibre failure as well as delamination. The sequence of these modes depends notably on different fibre architectures and loading conditions [5,6]. Based on these investigations, novel material models combining multiple failure criteria and continuum damage mechanics have been developed to describe the non-linear stress-strain behaviour of composite materials due to damage propagation under different loading conditions [7–10]. These models characterise the interactions between different failure modes as well as the resulting non-linear deformation process and are already applied to the study of diverse fibre- and textile-reinforced plastics [11,12]. Particularly, they are appropriately validated in experimental studies for specimens of a simple geometry and homogeneous loading conditions [5,13].

The gradual damage behaviour of composite materials, occurring from physical-based phenomena, results in local changes of stiffness and damping. This leads to a noticeable sequential alteration of the dynamic behaviour, specifically to a shift of the eigenfrequencies and of the modal damping ratio.

Composite rotors

For the description of the gradual damage behaviour of composite rotors, caused by operational loads or unpredicted loads such as impacts, verified damage mechanics models for composite materials are already available [5,14]. Typical failure modes for composite rotors are mainly inter-fibre failure from in-plane loads [15] and a mixture of inter-fibre failure, delaminations and fibre failure from unexpected impact loads [16], as depicted in Figure 1. However, the application of these damage mechanics models for rotor-typical loading conditions under consideration of the gradual damage behaviour and the resulting structural dynamic behaviour has not been thoroughly investigated.

Especially in aerospace industry, increasing economical demands in combination with high performance requirements have led to substantial breakthroughs in the design and development of high-speed composite rotors, such as rotor blades [17–20]. The main focus has been directed towards the in-plane and out-of-plane dynamic behaviour as well as the anisotropic material damping of undamaged composite rotors [21–25]. However, the gradual damage behaviour of composite rotors under unexpected loads has not been in the main scope of investigations of many researchers [26,27], and even less examined is the relation between gradual damage behaviour and corresponding dynamic behaviour of composite rotors.

Peer-reviewed version available at Materials 2018, 11, 2421; doi:10.3390/ma11122421

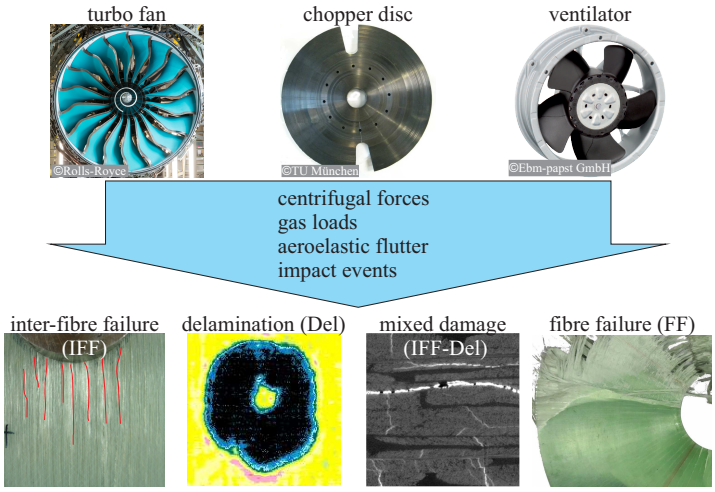

Figure 1. Examples of composites in the area of high performance rotors, in the area of turbofan aero engines, wind-turbines and ventilators and typical failure phenomena

Non-monotonic change of eigenfrequencies

A number of authors have reported a non-monotonic change of eigenfrequencies in composite structures. In particular the effect of low-impact-related delaminations are investigated [28,29] mainly due to local thickening accompanied by matrix cracking. Other similar investigations however did not identify this effect and reported a continuous reduction of the first eight eigenfrequencies with increasing delamination [30,31].

1.3. Aim and outline of the paper

Aim of the paper is to investigate the structural dynamic behaviour of composite rotors under propagating damage from a combination of out-of-plane and in-plane loads.

A thorough experimental work is performed, in order to investigate the gradual damage behaviour of composite rotors and the relation between damage and vibration behaviour. An elementary rotor geometry is selected with a representative fibre architecture for a CARTESIAN-orthotropic material behaviour. Consequently, a test matrix is defined including representative damage sequences and considering practice-relevant load conditions. Then, the rotors are investigated under initial damage as well as propagating damage, where both the resulting damage and the dynamic behaviour are estimated. The resulting damage is subsequently evaluated using a variety of non-destructive testing methods, in order to assess the type and extent of the inflicted damage.

For the determination of the dynamic behaviour of the composite rotors, experimental modal analysis tests are conducted, for which an impact excitation is achieved using an electrodynamic shaker with a mounted steel impactor. Finally, the damage-dependent dynamic behaviour of selected rotors is experimentally estimated and the results are presented and evaluated.

2. Composite disc rotors under rotor-typical load conditions

High-speed composite rotors undergo complex, inhomogeneous and variable stress conditions induced by centrifugal forces, which are mainly characterised by multi-axial tension and shear loads, as well as by further operational loads. The complex fibre-matrix architecture and its corresponding progressive damage behaviour increases the structural complexity, as shown in Figure 2. Furthermore, unpredicted impact loads can cause unexpected out-of-plane compression loads leading to inter-fibre failure and delaminations.

Preprints (www.preprints.org) | NOT PEER-REVIEWED | Posted: 8 November 2018 doi:10.20944/preprints201811.0191.v1

Peer-reviewed version available at Materials 2018, 11, 2421; doi:10.3390/ma11122421

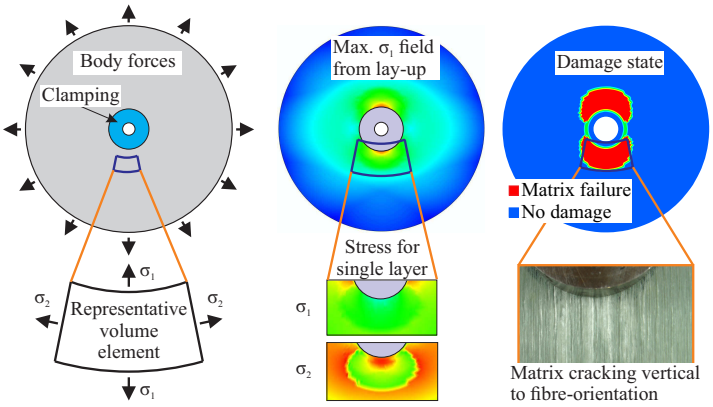

Figure 2. Rotor subjected to complex loading (left); data taken from a FEM model where the calculated stress field (centre) and in-plane anisotropic damage state (right)

2.1. Load-adapted fibre architectures

High-speed composite rotors using multi-axial non-crimp fabrics (NCF) as reinforcement are nowadays state of the art in the industry. A particular advantage of NCF in the field of textile semi-finished products are the absence of yarn crimping and a high variability. These advantages, in combination with a multilayer-manufacturing capability, makes this fabric type suitable for an efficient production of high-performance rotors. Another important feature of NCF is an adjustable damage behaviour that – in contrast to classical metallic materials – allows for a design of composite rotors with gradually progressing damage and predictable alterations of the resulting anisotropic material stiffness [26,32]. In particular, NCF offer high specific stiffness and strength as well as an adjustable energy absorption capacity. Currently, they are suited for various applications, with reported examples for composite chopper discs, saw discs and flywheels [33–36]. The investigation of rotors with a multi-axial fabric of endless glass fibres could therefore benefit the aforementioned industries.

2.2. Stress distribution

Problem-adapted semi-analytical calculation models have already been developed for the basic analysis of the deformation and failure behaviour of composite rotors [37]. These models provide an important contribution using elementary geometries, such as disc rotors for the development and optimisation of high-performance composite rotors. The structural analysis of CARTESIAN-orthotropic disc rotors can be achieved by means of closed mathematical solutions and for complex lay-ups using finite element methods, Figure 3.

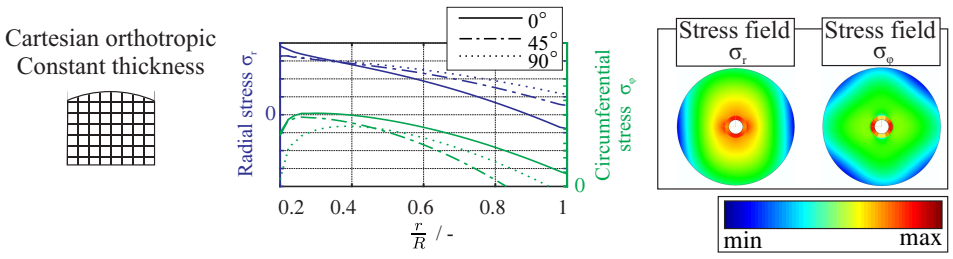

Figure 3. Illustration of rotors with different fibre architectures subjected to centrifugal forces; data taken from a finite element model with the calculated radial stress distribution (centre) and in-plane stress fields (right)

For the mathematical description of laminated rotors in CARTESIAN coordinates x, y, the methods of conformal mapping and complex stress functions are applied [38]. The resulting stress and displacement fields are dependent on the fibre orientation ϕ, which can be seen in the following relations,

Preprints (www.preprints.org) | NOT PEER-REVIEWED | Posted: 8 November 2018 doi:10.20944/preprints201811.0191.v1

Peer-reviewed version available at Materials 2018, 11, 2421; doi:10.3390/ma11122421

$$\sigma_i, u_j \sim \rho \cdot \omega^2 \cdot (x^2 + y^2) \tag{1}$$

$$\sigma_i, u_j = \mathcal{F}(\phi, \omega, \ldots) \tag{2}$$

with $\sigma_i = \sigma_x, \sigma_y, \tau_{xy}$ being the stress components, ρ the density, $u_j = u_x, v_y$ the displacement components and ω the angular velocity.

In the case of the CARTESIAN-orthotropic composite disc rotors, the structural behaviour can be determined on the basis of plane stress conditions, through the method of angle-preserving mapping and complex-valued stress functions. However, a rotationally symmetric load will result in a non-rotationally symmetrical stress state. Therefore, under complex in-plane loading from the centrifugal load σ_r^+, tensile stresses are mainly combined with intralaminar shear stresses (τ_{12}). This results in non-rotationally symmetrical damage evolution, mainly inter-fibre failure under different ply-dependent angles.

3. Material selection of fibre architecture and manufacturing of rotors

For the experimental investigation of the damage behaviour of composite rotors and their resultant dynamic behaviour a multi-ply multi-axial fabric is selected resulting in an in-plane CARTESIAN-orthotropic behaviour.

The selected NCF-fibre architecture is composed of a glass-fibre, non-crimp, multi-ply and multi-axial fabric [38]. The fabric reinforcement has an area density of 1.90 kg/m^2 and a ply thickness of 1 mm. Each of the $(0°, -45°, 90°, +45°)$ layers have a thickness of $(0.48, 0.23, 0.05, 0.23)$ mm, respectively. The composite lay-up consists of four such fabrics $[(0°/-45°/90°/+45°)/(-45°/90°/45°/0°)/(0°/-45°/90°/45°)/(-45°/90°/45°/0°)]$, as shown in Figure 4, resulting in a total laminate thickness of 4 mm. The inner and outer diameter of the rotor are 60 mm and 500 mm, respectively. The lay-up results in an in-plane orthotropic behaviour, and it is selected in order to achieve a polar non-symmetrical damage evolution caused by applied rotational loads. This material was extensively investigated in previous research projects, where the results indicated a gradual damage behaviour [39].

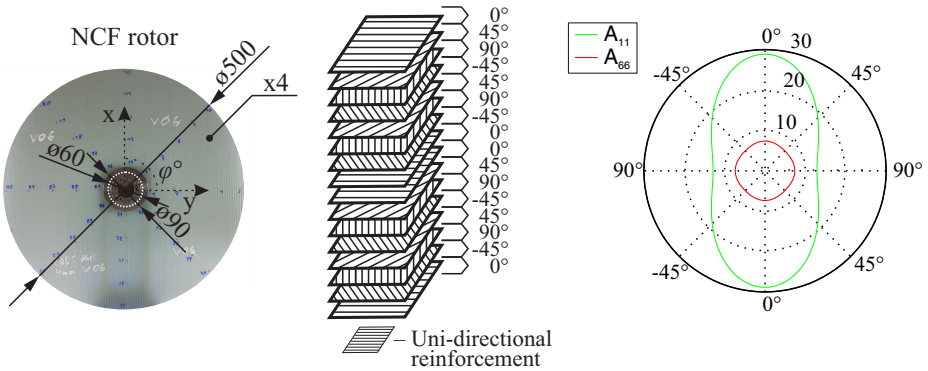

Figure 4. Geometry of a NCF rotor (left) with the lay-up (centre) and the corresponding homogenised directional stiffness properties A_{11}, A_{66}, resulting in an in-plane CARTESIAN-orthotropic behaviour (right)

A total of five NCF rotors are manufactured and their dynamic behaviour is experimentally investigated. The fabrication of the composite rotors is carried out using the state-of-the-art vacuum-assisted resin transfer moulding process, with the epoxy resin MGS-RIM-135 and process parameters similar to established investigations previously performed [39].

Preprints (www.preprints.org) | NOT PEER-REVIEWED | Posted: 8 November 2018 doi:10.20944/preprints201811.0191.v1

Peer-reviewed version available at Materials 2018, 11, 2421; doi:10.3390/ma11122421

4. Method for the investigation of representative damage sequences

The gradual damage evolution in a composite rotor throughout its entire designed operational lifetime includes both predicted and unpredicted load events, which can result in a structural failure before the end of its designed lifetime. A qualitative example of damage accumulation in a rotor under the influence of unpredicted events has been reported in [40]. The current approach utilises and further develops this work by specifying different load events. At first, an out-of-plane load is introduced, resembling an impact event, which results to an initial damage at different locations and with different load levels, as it is shown principally in Figure 5. Consequently, the composite rotor is run up to different rotational velocities, in order to induce further damage from increasing in-plane centrifugal loading.

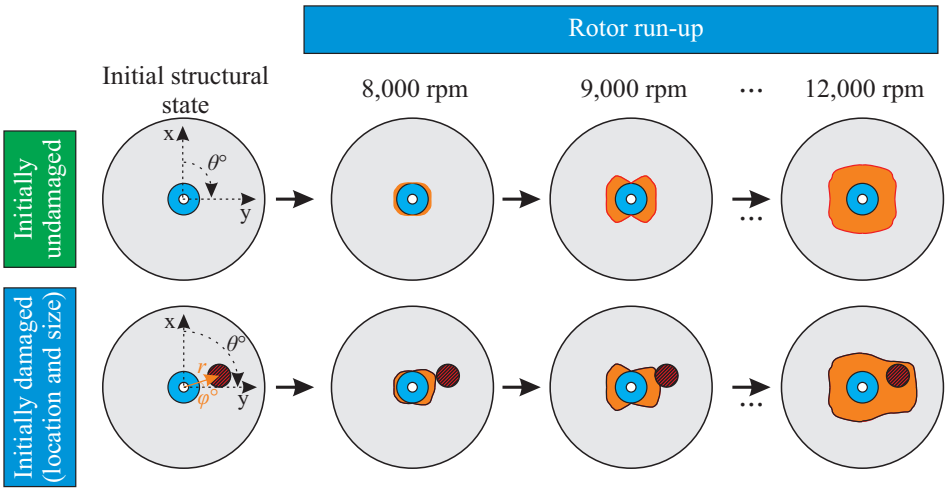

Figure 5. Illustration of two different damage sequences resulting from damage propagation during multiple rotor run-ups: one sequence without any initial damage (top), and one having an initial damage due to an out-of-plane load

Using such a combination of out-of-plane and in-plane loads, representative damage sequences can be generated with multiple structural states, for which their damage state and their dynamic behaviour can be investigated. At first, a sequence without initial damage is investigated at three nominally equal NCF rotors. Furthermore, two different sequences with the same initial damage at different positions are tested, each at a single NCF rotor. Each investigated rotor is run-up to different rotational velocities, as it is shown in Table 1.

Table 1. Overview of the experimentally investigated sequences for all types of rotors, with and without initial damage and under different rotational velocities

Name	**Initial damage** F (kN), r (mm), θ (°)	**Applied rotational velocity** 10^3 **rpm**										
		0	8	9	10	11	12	12.6	13	13.6	14	14.5
Rotor I.1	-	x	-	x	x	x	x	-	x	-	x	x
Rotor I.2	-	x	-	x	x	x	x	-	x	x	-	-
Rotor I.3	-	x	x	x	x	x	x	-	x	-	x	-
Rotor II	16, 100, 90	x	x	x	x	x	x	-	-	-	-	-
Rotor III	16, 100, 0	x	x	x	x	x	x	x	-	-	-	-

4.1. Determination of damage-initiating loads

In order to create rotor-typical damage from out-of-plane and in-plane loading, two damage-initiating loads are selected. Specifically, an out-of-plane compression load, and an in-plane centrifugal load are introduced, Figure 6.

Peer-reviewed version available at Materials 2018, 11, 2421; doi:10.3390/ma11122421

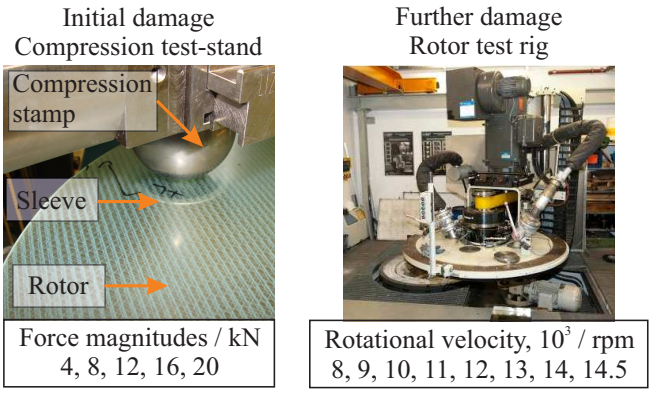

Figure 6. The compression test stand (left) and the rotor test rig (right) used for the sequential damage introduction

Out-of-plane compression loading for damage initiation

In order to introduce an impact-like damage in the rotors, a typical testing machine ZWICK equipped with a ball stamp and a sleeve base is used, as shown in Figure 6. The force-controlled testing machine presses the ball stamp and the rotor surface, in order to introduce barely visible damages in different regions of the investigated rotors. The ball stamp has a diameter of 80 mm, with a sleeve inner diameter of 63 mm and outer diameter of 75 mm. Five independent compression loads are applied with different load magnitudes between 4 kN and 20 kN, shown in Table 2.

Table 2. Overview of the applied parameters for the initial damage using a force-controlled compression test

Load parameters	Unit	Values
Introduced force	kN	4, 8, 12, 16, 20
Test speed	mm/min	2
Compression stamp diameter	mm	80
Sleeve inner diameter	mm	63
Sleeve outer diameter	mm	75

In-plane loading from multiple rotor run-ups for damage propagation

In-plane loading is experimentally introduced by sequential run-ups of the rotor, using the available high-speed rotor test rig BI4U at the ILK, shown in Figure 6. In order to avoid any change of the temperature-dependent material properties of the matrix caused by friction between the rotor and the air, a technical vacuum is applied in the range of 2.4 mbar and 2.7 mbar.

The damage initiation of NCF rotors is approximately determined at 8,000 rpm at progressive run-up tests, in which the rotors are run up in steps of 1,000 rpm. The rotors are first accelerated to 8,000 rpm with an angular acceleration of 3 rad/s^2, then rotated at the defined speed for a time period of 120 s and subsequently decelerated with 3 rad/s^2 to a stand-still. With every run-up, the body forces increase, causing the propagation of in-plane damage at the rotors.

The used rotor test rig is mounted with a fail-safe monitoring system, causing an automatic shut down of the test rig, when a shaft vibration of 350 µm is reached. Due to the propagating damage, different imbalances accumulate for the two rotor-types, which are reflected as increasing vibration values in the shaft, respectively. Therefore, the NCF rotors are sequentially run-up with steps of 1,000 rpm until the rotor test rig is automatically shut down due to a shaft vibration of 350 µm.

For the NCF rotor I.1, without any initial damage, the test is completed at 14,500 rpm and similar for the NCF rotors I.2 and I.3 at 14,000 rpm, see Table 1. However, for the NCF rotors II and III, which have an initial damage, the rotor test rig is shut down at 12,000 rpm and 12,600 rpm, respectively.

Peer-reviewed version available at Materials 2018, 11, 2421; doi:10.3390/ma11122421

Table 3. Overview of the identified resulting damage for both loading types

Loading type	Resulting damage
Initial out-of-plane compression	Inter-fibre cracks Delamination Isolated fibre cracks at 20 kN
Centrifugal in-plane loading	Inter-fibre cracks Spatial inter-fibre crack distribution

4.2. Evaluation of the inflicted damage

A variety of non-destructive evaluation methods are applied in order to perform a phenomenological assessment of the type and extent of the inflicted damage. The characterisation of the initial damage and the propagating damage is performed, and the predominant failure modes are identified for every case. Three non-destructive evaluation methods are applied with each method identifying different aspects of the failure modes, and with a measurement resolution on the µm scale:

- High-resolution visual inspection for the identification of spatial inter-fibre cracks due to the in-plane load.
- Ultrasonic testing for the evaluation of the form and size of delaminations,
- Computer tomography for the identification of single inter-fibre failures, resin-rich areas, and the number of delaminations through the thickness.

High resolution optical inspection

As the fibre architecture has a refraction index similar to that of the epoxy matrix, which amounts to 1.548 - 1.552, it is possible to use optical inspection to identify the inflicted damage [22]. A high-resolution optical camera NIKON D3100 is therefore used with an optical resolution of 4608 × 3072 pixel. After each applied loading, the state of the rotor is photographically documented in order to capture the inflicted damage.

The transparency of the investigated composite rotors allows for the monitoring of both the crack densities and the existence of delaminations from the initial impact using the optical method with a high-resolution camera, as it is shown in Figure 7. At low magnitudes, up to 4 kN, a small damage is observed and an increase of the delaminated area is observed between 8 kN through 16 kN. For a magnitude of 20 kN the applied delamination has the same area as in the case of 16 kN.

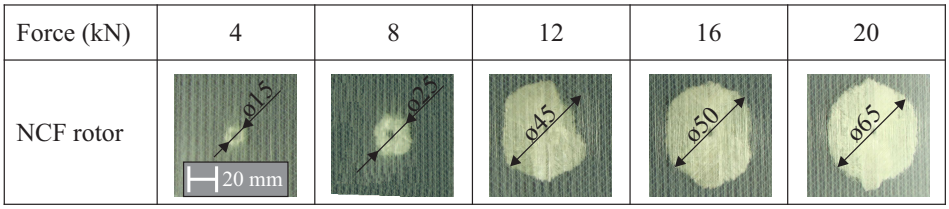

Figure 7. Optical resolutions of five different delaminated areas for a NCF rotor of five different load magnitudes

By using the photographically documented damaged states of different areas of a NCF rotor, inter-fibre cracks are identified in the respective main fibre orientations, as shown in Figure 8. Under increasing damage, inter-fibre cracks further develop in each layer and they become visible as crack lines in their respective directions. All rotors exhibit the same damage initiation due to run-up, specifically inter-fibre damage, at similar rotational velocities due to the used matrix system. The selected fibre architecture of the NCF rotors and the corresponding CARTESIAN-orthotropic material behaviour results in a non-rotational symmetrical damage propagation, as shown in Figure 8.

Preprints (www.preprints.org) | NOT PEER-REVIEWED | Posted: 8 November 2018 doi:10.20944/preprints201811.0191.v1

Peer-reviewed version available at Materials 2018, 11, 2421; doi:10.3390/ma11122421

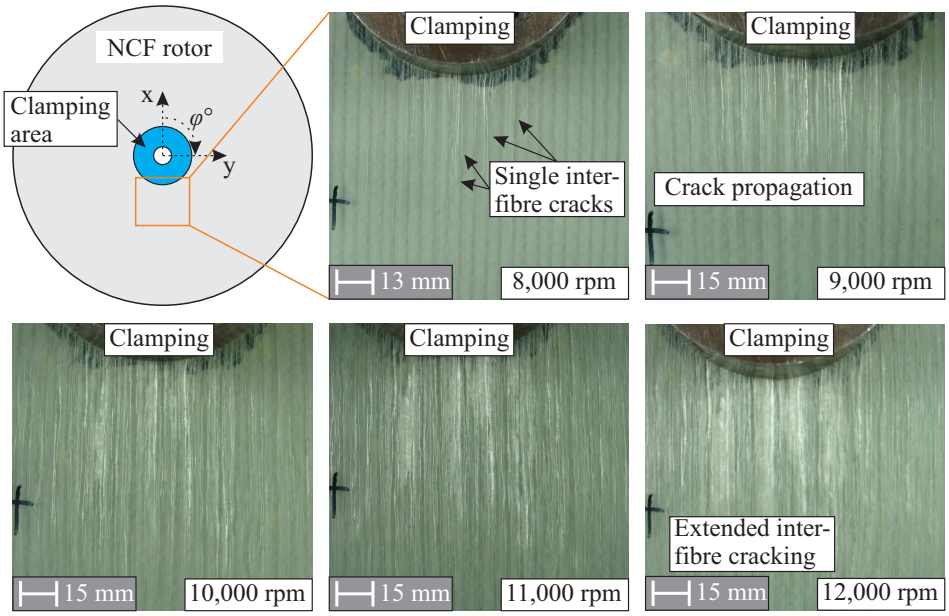

Figure 8. Typical damage due to a run-up of a NCF rotor after different rotational velocities, resulting in an increasing number of spatial matrix damage

Ultrasonic testing for the evaluation of delaminations

The set-up for the ultrasonic testing is shown in Figure 9 (left), where a NCF rotor is clamped at four points and an air-coupled ultrasonic test takes place in a modular ultrasonic inspection system from the company Dr. HILLGER, type AirTech-4000, with a maximum resolution of 125 µm.

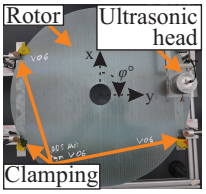

Force / kN	4	8	12	16	20
NCF rotor	20 mm				

Figure 9. Overview of the ultrasonic results after out-of-plane compression loads with different force magnitudes for NCF-rotors where the formation of delaminations is observed by 8 kN

Due to the increased inherent material damping of composites, the testing range is approximately 250 kHz. As a result, the spatial resolution is decreased, making ultrasonic testing more suitable for delamination investigation than for single, isolated inter-fibre failures [41]. Therefore, inter-fibre cracks and fibre fracture paths are difficult to detect, because their reflecting surface is not wide enough in contrast to delaminations [42].

The relationship between the investigated compression loads and the resulting damaged area is shown in Figure 9. Clearly distinguishable damage regions are highlighted by the black and blue colour in the ultrasonic images. Based on these results, the delamination shape is quantified as a circular area. The position of the delamination through the thickness and the existence of multiple delaminations are already determined using the subsequently presented computer tomography scans.

Computer tomography investigations

Computer tomography (CT) is predestined for the material assessment of composites as it is a non-destructive approach, which provides a measurement resolution in µm. Therefore, CT scans are taken for the identification of single inter-fibre failures, resin-rich areas, and the number of delaminations. In this work, conventional investigations are performed using a CT machine NANOTOM 180 NF from the company GE SENSING & INSPECTION TECHNOLOGIES.

Peer-reviewed version available at Materials 2018, 11, 2421; doi:10.3390/ma11122421

The applied in-plane loads result in the formation of inter-fibre cracks, as shown in Figure 10. In the case of the damaged NCF rotor III due to an applied rotational velocity of 12,000 rpm, an extended inter-fibre cracking in multiple layers is observed transversely to the main fibre orientation, as shown in Figure 10 (top). The inter-fibre cracks are distributed among many layers of the lay-up.

For the damaged NCF rotor III due to an out-of-plane compression load of 16 kN, the characteristic failure types are identified as delaminations and inter-fibre cracks, as shown in Figure 10 (bottom). A main delamination is formed for the NCF rotors near the middle position of the lay-up. Furthermore, multiple smaller delaminations and inter-fibre cracks are evident between the layers.

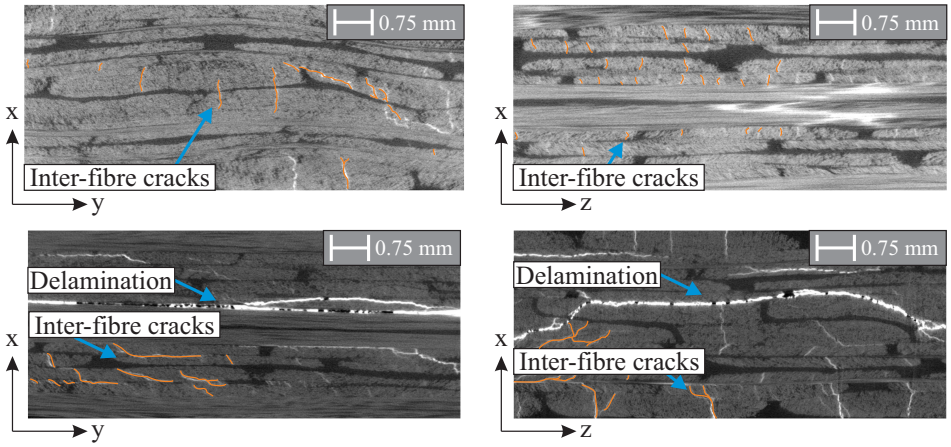

Figure 10. Computer tomography picture of a NCF rotor after an in-plane load and the corresponding damage, where inter-fibre cracks are identified as the predominant failure mode (top); and with an initial damage caused by a compression load of 16 kN resulting mainly to delaminations and inter-fibre cracks (bottom)

Identification of predominant failure modes

A mixture of different failure modes are identified for both loading conditions. An overview of the identified resulting damage is shown in Table 3. Notably, propagating damage due to rotor run-up starts approximately at 40 % of the maximum applied in-plane load, and comprises mainly inter-fibre cracks. Fibre failure is not detected until the total failure of the rotors and the gradual damage behaviour is confirmed for all rotors.

5. Results and discussion of the investigated dynamic behaviour of composite rotors

The damage-dependent dynamic behaviour of the investigated rotors is experimentally estimated and selected results are presented. For each investigated damage state, an experimental modal analysis is performed using a self-developed excitation system combined with a contactless Laser-Scanning-Vibrometer (LSV) (POLYTEC, Type PSV-400).

5.1. Experimental modal analysis

For the excitation with respect to modal analysis, an optimised burst signal is sent to an electrodynamic shaker, where a steel impactor and a force sensor is mounted, as shown in Figure 11, causing a stroke of the impactor. In this way, double hits are eliminated and excitation uncertainties are reduced, which is a main advantage by impact hammer modal analysis. A further advantage of the developed excitation is the reproducibility. Between sequential measurements from the force sensor a deviation of 0.1 % has been calculated showing a precise excitation capability.

For acquiring the vibration response and the resulting mode shapes of each eigenfrequency, the roving measurement point method is selected for the measurement of the resultant vibration response due to the existing equipment: the developed combined excitation system and the LSV [43].

Preprints (www.preprints.org) | NOT PEER-REVIEWED | Posted: 8 November 2018 doi:10.20944/preprints201811.0191.v1

Peer-reviewed version available at Materials 2018, 11, 2421; doi:10.3390/ma11122421

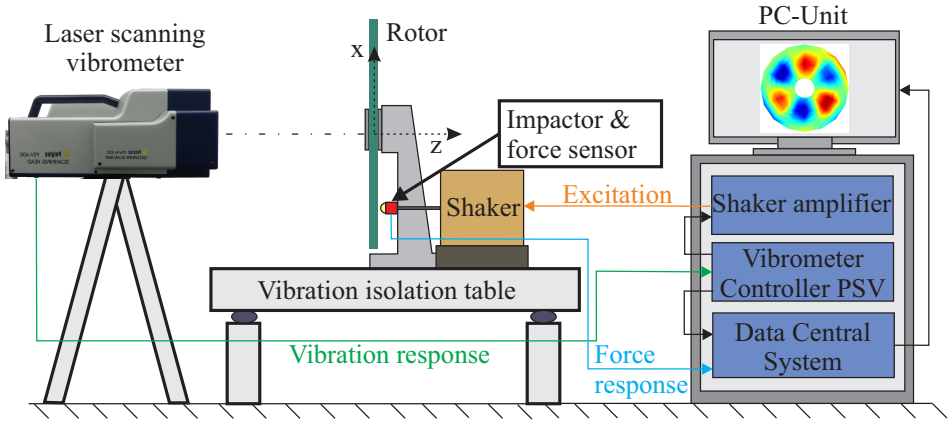

Figure 11. Experimental set-up for the modal analysis of clamped composite rotors; the impact excitation is achieved using an electrodynamic shaker with a mounted steel impactor; the vibration response measurement using a Laser-Scanning-Vibrometer (POLYTEC, Type PSV-400)

For the experimental estimation of the vibration response of each rotor, a pattern of 128 measuring points is defined, as shown in Figure 12. This number of measuring points serves to experimentally determine local mode shapes at higher frequencies.

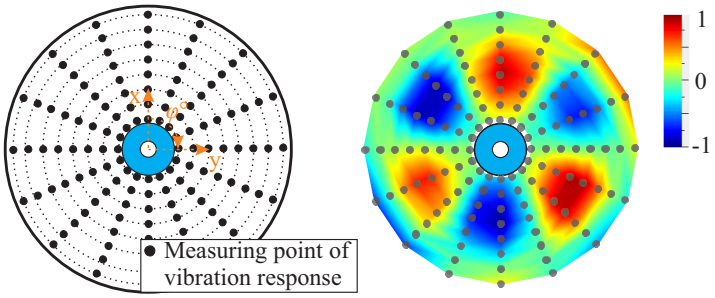

Figure 12. Measuring mesh with a pattern of 128 measuring points for the determination of the vibration response of each rotor (left) and an experimentally determined mode shape (3,1,0) with colour plot of the normalised measured surface speed (right)

Based on the position of the measurement points, different components of the vibration response are measured using the LSV, providing information regarding the excited eigenfrequencies at the measured points, with selected settings shown in Table 4. As measured signals are superimposed with noise, subsequent measurements are taken and magnitude averaging is implemented to reduce the noise to signal ratio. For each determined response of N samples, the magnitudes of their complex values are calculated, added and subsequently divided by N, as shown in Equation 3 [43]:

$$\overline{P}_{yy} = \frac{1}{N} \cdot \sum_{i=1}^{N} \left| P_{yy}(i) \right| \quad . \tag{3}$$

Table 4. Overview of the applied settings for the experimental modal analysis

Setting parameters	Selected setting
Measuring points	128
Type of excitation	Impact
Sample frequency	6.4 kHz
FFT settings	Triple magnitude averaging, 2.5 kHz, 12,800 lines, rectangular window
Type of vibrometer	POLYTEC, Type PSV-400

Peer-reviewed version available at Materials 2018, 11, 2421; doi:10.3390/ma11122421

5.2. Assessment of the damage-dependent dynamic behaviour

The relation between applied in-plane loads and the corresponding shift of eigenfrequencies due to damage increase is investigated for five different damage sequences. For each damage sequence, a total of 16 eigenfrequencies are investigated for five NCF rotors. For each type of rotor, a normalised in-plane load $F_c^{'}$ is introduced,

$$F_c^{'} = \left(\frac{n_{rpm}}{n_{rpm}^{max}} \right)^2 \tag{4}$$

where each rotational velocity n_{rpm} is divided from the maximum achieved rotational velocity n_{rpm}^{max} for each sequence, as it was shown previously in Table 1.

The frequency shift for each eigenfrequency EF_i is determined for each damage state S_j under a rotational in-plane load, as

$$\Delta f(EF_i|S_j) = f(EF_i|S_j) - f(EF_i|S_0), \tag{5}$$

where $EF_i|S_j$ is the eigenfrequency at the S_j state, and $EF_i|S_0$ is the eigenfrequency value at the S_0 state. For the two damage sequences where multiple rotors have been investigated, i.e. NCF rotor I, a mean frequency shift is calculated and fitted using a third-degree polynomial.

Two different types of frequency shifts for each EF can be observed for all investigated damage sequences, as shown in Figure 13 for four typical eigenmodes. First, the eigenfrequencies of the mode shapes (1,1,90) and (4,1,0) remains constant and slightly increases, followed with a typical frequency decrease under the increase of damage, Figure 13 (right).

However, a different behaviour is exhibited for the eigenfrequencies of the mode shapes (2,0,0) and (4,0,0). First, the frequency increases, and with increasing damage it reaches a maximum, as shown in Figure 13 (left). Then, with further damage increase, the eigenfrequency change decreases. The aforementioned behaviour between different types of eigenmodes is visible for both sequences without initial damage, NCF-rotor I and with initial damage, NCF-rotor II and NCF-rotor III and for other investigated eigenmodes.

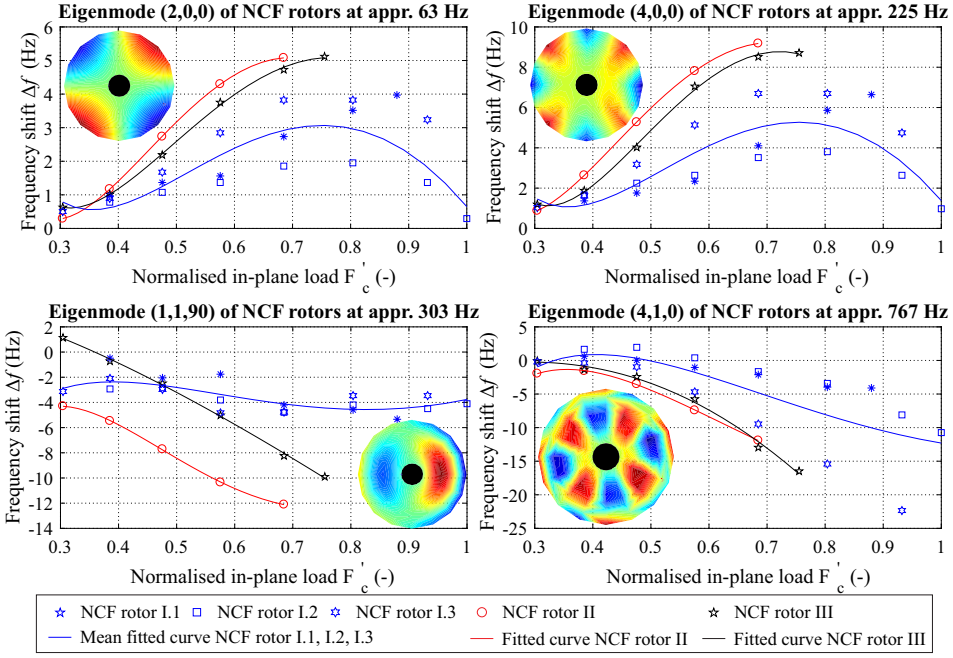

Figure 13. Shift of the eigenfrequencies of all investigated NCF rotors for two eigenmodes shown as an example: one with a non-monotonic change of the eigenfrequency (left) and one with a monotonic decrease of the eigenfrequency (right)

Based on these results, it can be deduced that a monotonic increase of damage can result in a non-monotonic frequency change of 10 out of 18 eigenfrequencies, a percentage of 55 % of all investigated eigenmodes, as shown in Figure A1 and Figure A2 .

This effect is observed for all investigated sequences, with and without initial damage. Numerical investigations show that the reasons for the non-monotonic behaviour can be coupling effects, a combination of pre-stress effects from the curing process, the occurring type of damage propagation combined with the geometry, and specific mode shapes.

6. Conclusions

A thorough experimental investigation is conducted, in order to analyse the gradual damage behaviour of composite rotors. Representative damage sequences are generated by applying both in-plane and out-of-plane loads, and are considered as sequences of distinct structural damage states. It is experimentally identified that the investigated composite rotors are damaged by the applied forces, but that they are still operational after a substantial extent of inter-fibre failure.

For the experimental damage identification, a number of investigations are performed for each generated structural state. Firstly, non-destructive testing is applied in order to identify the inflicted damage. Based on three different non-destructive evaluation methods, the damage is evaluated, and predominant failure types are identified and described. Then the estimation of the structural dynamic behaviour is performed using experimental modal analysis, and the modal properties are determined for each damage state. A novel observation is reported finding that a monotonic increase of damage can result in a non-monotonic frequency shift of a significant amount of eigenfrequencies for all investigated rotors.

This work provides the basis for further, detailed investigation of composite structures regarding the non-monotonic change of eigenfrequencies for different fibre architectures, loading and boundary conditions.

Funding: The authors would like to express their gratitude for the financial support from the Deutsche Forschungsgemeinschaft (funding code GU 614/14-1).

Conflicts of Interest: The authors declare no conflict of interest.

Abbreviations

The following abbreviations are used in this manuscript:

NCF	Non-crimp fabric
FEM	Finite element model
ILK	Institute of Lightweight Engineering and Polymer Technology
CT	Computer tomography
LSV	Laser-scanning vibrometer
EF	Eigenfrequency

Appendix. Experimentally determined frequency shift of investigated NCF rotors

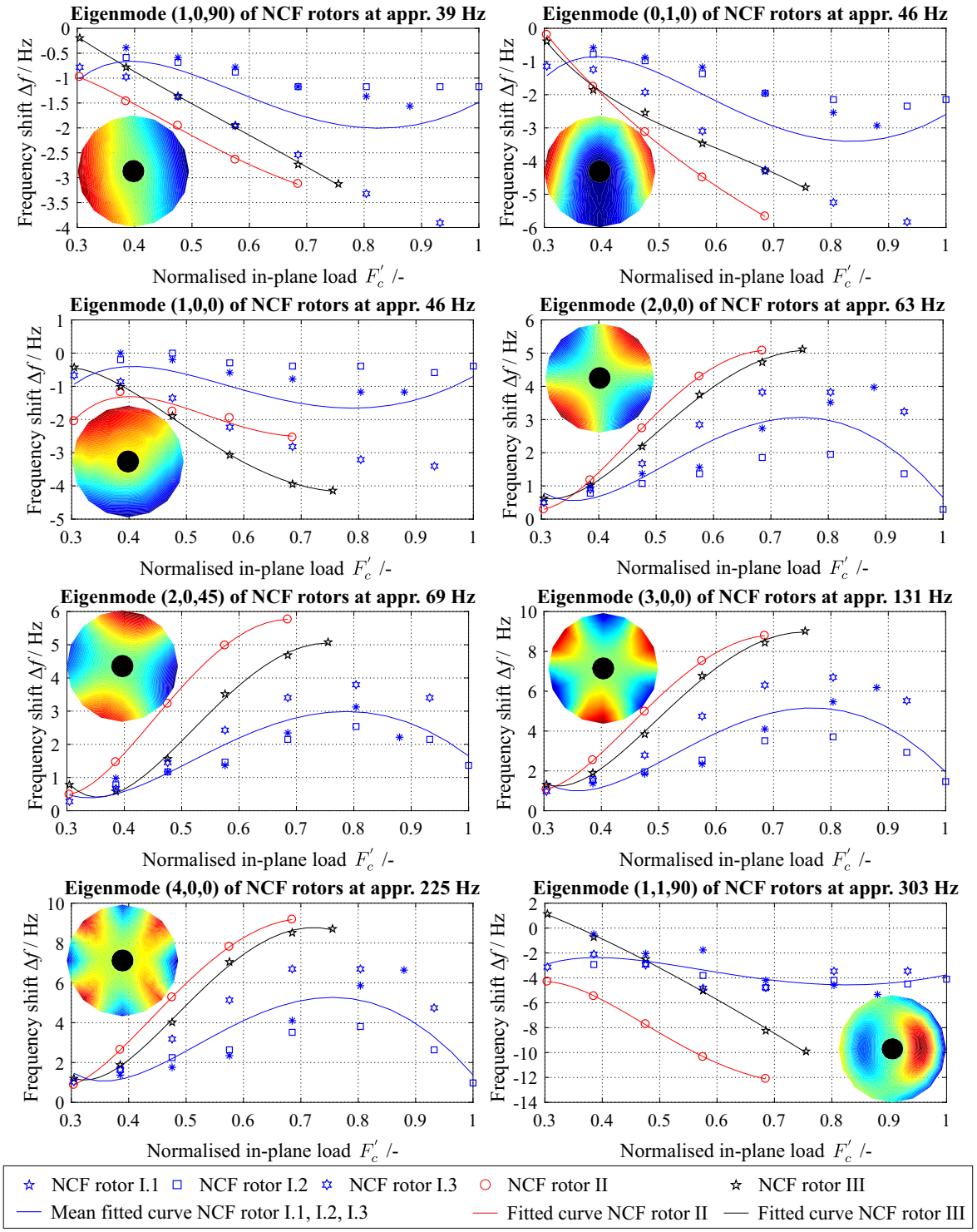

Figure A1. Experimentally determined frequency shift of investigated NCF rotors

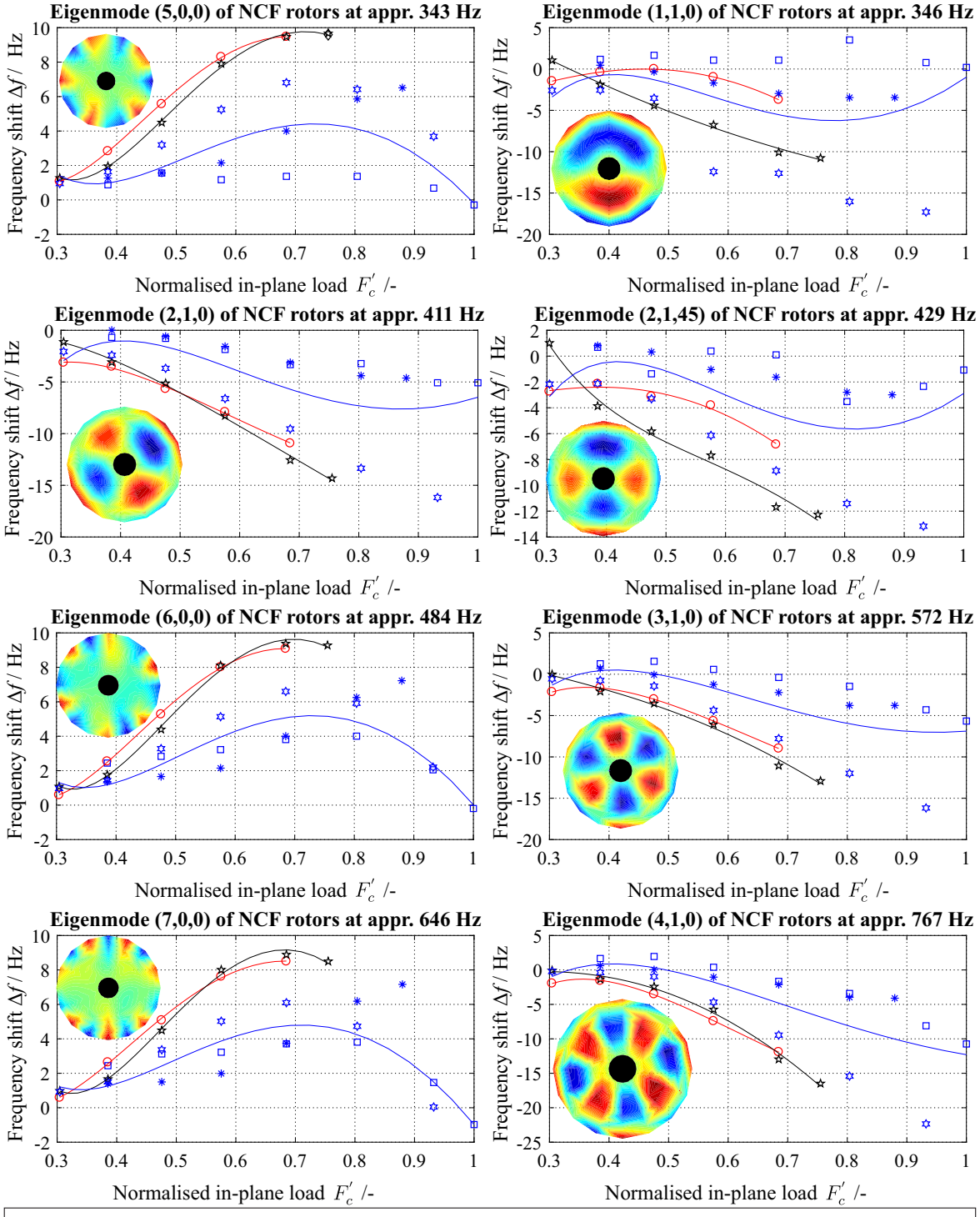

Figure A2. Experimentally determined frequency shift of investigated NCF rotors

Peer-reviewed version available at Materials 2018, 11, 2421; doi:10.3390/ma11122421

References

1. Puck, A.; Schürmann, H. Failure analysis of FRP laminates by means of physically based phenomenological models. *Composites Science and Technology* **1998**, *58*, 1045–1067.
2. Hashin, Z. Failure criteria for unidirectional fiber composites. *Journal of Applied Mechanics Transactions of the ASME* **1980**, *47*, 329–334.
3. Hinton, M.J.; Kaddour, A.S.; Soden, P.D. *Failure criteria in fibre reinforced polymer composites: the world-wide failure exercise*; Elsevier, 2004.
4. Hufenbach, W.; Petrinic, N.; Gude, M.; Langkamp, A.; Andrich, M. *Experimentelle Versagensanalyse von textilverstärkten Verbundwerkstoffen bei hochdynamischer Belastung*; Wiley-VCH Verlag GmbH & Co. KGaA, 2006.
5. Böhm, R.; Hufenbach, W. Experimentally based strategy for damage analysis of textile-reinforced composites under static loading. *Composites Science and Technology* **2010**, *70*, 1330–1337.
6. Hufenbach, W.; Gude, M.; Thieme, M.; Böhm, R. Failure behaviour of textile reinforced thermoplastic composites made of hybrid yarns-II: Experimental and numerical studies. ICF12 Ottawa 2009, 2013, pp. 1–10.
7. Böhm, R.; Gude, M.; Hufenbach, W. A phenomenologically based damage model for 2D and 3D-textile composites with non-crimp reinforcement. *Materials & Design* **2011**, *32*, 2532–2544.
8. Thieme, M.; Böhm, R.; Gude, M.; Hufenbach, W. Probabilistic failure simulation of glass fibre reinforced weft-knitted thermoplastics. *Composites Science and Technology* **2014**, *90*, 25–31.
9. Gude, M.; Schirner, R.; Weck, D.; Dohmen, E.; Andrich, M. Through-thickness compression testing of fabric reinforced composite materials: Adapted design of novel compression stamps. *Polymer Testing* **2016**, *56*, 269 – 276.
10. Bui, V.Q.; Iannucci, L.; Robinson, P.; Pinho, S.T. A coupled mixed-mode delamination model for laminated composites. *Journal of Composite Materials* **2011**, *45*, 1717–1729.
11. Gude, M.; Freund, A.; Vogel, C.; Kupfer, R. Simulation of a Novel Joining Process for Fiber-Reinforced Thermoplastic Composites and Metallic Components. *Mechanics of Composite Materials* **2017**, *52*, 733–740.
12. Zscheyge, M.; Gude, M.; Böhm, R.; Hufenbach, W. Strain rate dependent deformation and damage behavior of textile-reinforced thermoplastic composites. 2016.
13. Böhm, R.; Gude, M.; Hufenbach, W. A phenomenologically based damage model for textile composites with crimped reinforcement. *Composites Science and Technology* **2010**, *70*, 81–87.
14. Filippatos, A.; Höhne, R.; Kliem, M.; Gude, M. A composite-appropriate integration method of thick functional components in fibre-reinforced plastics. *Smart Materials and Structures* **2016**, *25*, 035026.
15. Kuschmierz, R.; Filippatos, A.; Günther, P.; Langkamp, A.; Hufenbach, W.; Czarske, J.; Fischer, A. In-process, non-destructive, dynamic testing of high-speed polymer composite rotors. *Mechanical Systems and Signal Processing* **2015**, *54-55*, 325–335.
16. Chang, F.K. *Structural health monitoring 2000*; CRC Press, 1999.
17. Red, C. Aviation outlook: Composites in commercial aircraft jet engines. *High-Performance Composites* **2008**.
18. Ghorashi, M.; Nitzsche, F. Nonlinear dynamic response of an accelerating composite rotor blade using perturbations. *Journal of Mechanics of Materials and Structures* **2009**, *4*, 693–718.
19. Klaeger, U.; Galazky, V. Novel concept for manufacturing lightweight centrifuge rotors for laboratories. 5^{th} International Virtual and Physical Prototyping Conference, 2011, pp. 763–766.
20. Middleton, D. *Composite materials in aircraft structures*; John Wiley & Sons, Incorporated, 1990.
21. Duffy, K.P.; Choi, B.B.; Provenza, A.J.; Min, J.B.; Kray, N. Active piezoelectric vibration control of subscale composite fan blades. *Journal of Engineering for Gas Turbines and Power* **2013**, *135*, 011601.
22. Gude, M.; Filippatos, A.; Langkamp, A.; Hufenbach, W.; Kuschmierz, R.; Fischer, A.; Czarske, J. Model assessment of a composite mock-up bladed rotor based on its vibration response and radial expansion. *Composite Structures* **2015**, *124*, 394–401.
23. Chang, S.H.; others. Performance of high speed air spindle motor equipped with composite squirrel cage rotor. *Composite Structures* **2002**, *55*, 419–427.
24. Philipp, K.; Filippatos, A.; Kuschmierz, R.; Langkamp, A.; Gude, M.; Fischer, A.; Czarske, J. Multi-sensor system for in-situ shape monitoring and damage identification of high-speed composite rotors. *Mechanical Systems and Signal Processing* **2016**.

25. Oberholster, A.J.; Heyns, P.S. Online condition monitoring of axial-flow turbomachinery blades using rotor-axial Eulerian laser Doppler vibrometry. *Mechanical Systems and Signal Processing* **2009**, *23*, 1634–1643.
26. Hufenbach, W.; Langkamp, A.; Kostka, P.; Böhm, R. Damage behaviour of high speed textile reinforced composite rotors. *Kompozyty-Composites* **2005**, *2*, 23–28.
27. Pawar, P.M.; Ganguli, R. On the effect of progressive damage on composite helicopter rotor system behavior. *Composite Structures* **2007**, *78*, 410–423.
28. Hou, J.P.; Jeronimidis, G. Vibration of delaminated thin composite plates. *Composites Part A: Applied Science and Manufacturing* **1999**, *30*, 989–995.
29. Hou, J.P.; Jeronimidis, G. Bending stiffness of composite plates with delamination. *Composites Part A: Applied Science and Manufacturing* **2000**, *31*, 121–132.
30. Valdes, S.D.; Soutis, C. Delamination detection in composite laminates from variations of their modal characteristics. *Journal of Sound and Vibration* **1999**, *228*, 1–9.
31. Lee, S.; Park, T.; Voyiadjis, G.Z. Vibration analysis of multi-delaminated beams. *Composites Part B: Engineering* **2003**, *34*, 647–659.
32. Hufenbach, W.; Gude, M.; Ebert, C. Hybrid 3D-textile reinforced composites with tailored property profiles for crash and impact applications. *Composites Science and Technology* **2009**, *69*, 1422–1426.
33. Weinzierl, M.; Schatz, M.; Antonelli, V.; Baier, H. Structural design optimization of CFRP chopper disks. *Composite Structures* **2016**, *140*, 351–359.
34. Lowder, J. Composite circular saw blade, 2006. US Patent App. 11/218,732.
35. Kullmann, J.H. Cfk-sägeblatt, 2015. WO Patent App. PCT/EP2013/068 001.
36. Ratner, J.K.H.; Chang, J.B.; Christopher, D.A. *Flywheel rotor safe-life technology: Literature search summary*; Vol. 2002-211810, *NASA CR*, National Aeronautics and Space Administration, Glenn Research Center, 2002.
37. Müller, C.H. *Grundlagen zur Entwicklung scheibenförmiger Hochleistungsrotoren aus Faser-Kunstoff-Verbunden*; Dissertation, Technische Universität Clausthal, 1993.
38. Hufenbach, W.; Kroll, L.; Grothaus, R. New design methods for complexly loaded high-speed composite rotors. 8^{th} European Conference on Composite Materials, 1998, pp. 511–518.
39. Hufenbach, W.; Köhler, K. *Textile Verbundbauweisen und Fertigungstechnologien für Leichtbaustrukturen des Maschinen- und Fahrzeugbaus*; Technische Universität Dresden, 2008.
40. Hufenbach, W.; Fidali, M.; Kostka, P.; Langkamp, A. Influence of embedded diagnostic sensors on structural dynamic behaviour of composite rotors. *Kompozyty-Composites* **2006**, pp. 14–19.
41. Hosur, M.V.; Murthy, C.R.; Ramamurthy, T.S.; Shet, A. Estimation of impact-induced damage in CFRP laminates through ultrasonic imaging. *NDT & E International* **1998**, *31*, 359–374.
42. Aymerich, F.; Meili, S. Ultrasonic evaluation of matrix damage in impacted composite laminates. *Composites Part B: Engineering* **2000**, *31*, 1–6.
43. Polytec GmbH, Waldbronn. *Theory manual of Polytec scanning vibrometer*, edition 8 ed., 2010.